

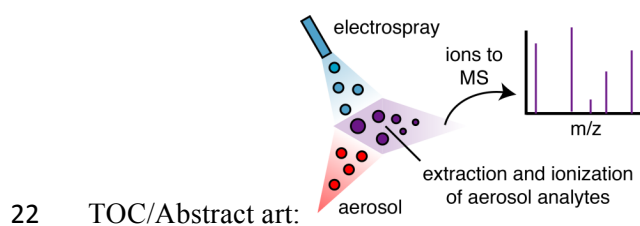
1 **Characterising an Extractive Electrospray Ionisation (EESI) source for the online mass**  
2 **spectrometry analysis of organic aerosols**

3 Peter J. Gallimore and Markus Kalberer\* (corresponding author: [markus.kalberer@atm.ch.cam.ac.uk](mailto:markus.kalberer@atm.ch.cam.ac.uk))

4 Department of Chemistry, University of Cambridge, Lensfield Road, Cambridge, CB2 1EW, UK

6 **Abstract**

7 Organic compounds comprise a major fraction of tropospheric aerosol and understanding their  
8 chemical complexity is a key factor for determining their climate and health effects. We present and  
9 characterise here a new online technique for characterising the detailed chemical composition of  
10 organic aerosols, namely Extractive Electrospray Ionisation Mass Spectrometry (EESI-MS). Aerosol  
11 particles composed of soluble organic compounds were extracted into and ionised by a solvent  
12 electrospray, producing molecular ions from the aerosol with minimal fragmentation. We demonstrate  
13 here that the technique has a time resolution of seconds and is capable of making stable measurements  
14 over several hours. The ion signal in the MS was linearly correlated with the mass of aerosol  
15 delivered to the EESI source over the range tested ( $3\text{-}600\ \mu\text{g}/\text{m}^3$ ) and was independent of particle size  
16 and liquid water content, suggesting that the entire particle bulk is extracted for analysis. Tandem MS  
17 measurements enabled detection of known analytes in the sub- $\mu\text{g}/\text{m}^3$  range. Proof-of-principle  
18 measurements of the ozonolysis of oleic acid aerosol ( $20\ \mu\text{g}/\text{m}^3$ ) revealed the formation of a variety of  
19 oxidation products in good agreement with previous offline studies. This demonstrates the technique's  
20 potential for studying the product-resolved kinetics of aerosol-phase chemistry at a molecular level  
21 with high sensitivity and time resolution.



## 1 **Introduction**

2 Aerosols have an important influence on climate both directly by light scattering and indirectly by  
3 influencing cloud formation and cloud processes, through their ability to act as cloud condensation  
4 nuclei and ice nuclei.<sup>1</sup> Particulate matter also has significant negative health effects, with exposure to  
5 fine-particulate air pollution linked to respiratory and cardiovascular disease<sup>2</sup> and reduced life  
6 expectancy.<sup>3</sup>

7

8 Organic compounds are often the dominant fraction of tropospheric aerosol.<sup>4</sup> Despite this, our  
9 understanding of the sources, formation processes and atmospheric properties of organic aerosol is  
10 limited.<sup>5</sup> There is increasing recognition that reactions occurring in the condensed phase are altering  
11 the particle composition continuously during its lifetime and are key to explaining observed aerosol  
12 yields and composition.<sup>6</sup> A lack of detailed knowledge of their chemical composition is regarded as a  
13 limiting factor in understanding their effect on the climate and human health. One of the main  
14 challenges for the analysis of organic aerosols is their complex composition; up to several thousand  
15 compounds have to be separated.<sup>7</sup> In addition, there are usually only trace amounts of sample  
16 available for analysis, often in the nanogram range. Furthermore, atmospheric aerosol composition is  
17 often changing very rapidly, favouring fast-response online analytical-chemical techniques. In  
18 general, mass spectrometry techniques are well suited to measure highly complex samples at trace  
19 concentrations.

20

21 Established mass spectrometry techniques for characterising the composition of organic aerosols fall  
22 broadly into two categories; “online” measurements where particles are analysed in real time, and  
23 “offline” methods where particles are first collected and subsequently processed for analysis. Online  
24 particle analysis can be performed using instruments such as the aerosol mass spectrometer (AMS)<sup>8</sup>  
25 which employs thermal desorption/electron ionisation, or with laser desorption/ionisation (LDI)  
26 techniques such as aerosol time-of-flight MS.<sup>9</sup> These instruments are sensitive to ambient aerosol

1 concentrations but extensive fragmentation of the organic components is common due to the high  
2 energy ionisation conditions. Therefore, identifying specific compounds is a difficult task. Recent  
3 instrumental developments are concentrating on “softer” laser ionisation techniques to reduce  
4 compound fragmentation, such as near-IR LDI<sup>10</sup> and photo-ionisation AMS.<sup>11</sup> Vogel et al.<sup>12</sup> have  
5 recently measured organic acids in boreal forest aerosols using atmospheric pressure chemical  
6 ionisation.

7

8 A variety of offline analytical techniques have been used to characterise aerosol samples collected  
9 onto filters or impactors.<sup>13</sup> The disadvantage of offline techniques is that after an extended sample  
10 collection period (typically hours) where the aerosol chemical composition may change due to  
11 evaporation or reaction of components, extracting material from the substrate can be time-consuming  
12 and introduce further artefacts into the resulting measurements.<sup>14</sup> The low time-resolution also often  
13 limits the use of offline techniques for atmospheric studies where many processes have time scales of  
14 seconds to minutes.

15

16 A number of new offline techniques overcome the need for an extraction step by directly sampling  
17 collected aerosol from the substrate surface. Desorption electrospray ionisation<sup>15</sup> has proved useful in  
18 analysing both field and laboratory samples and is especially suitable for characterising labile  
19 compounds and particles subjected to chemical aging. Bruns et al.<sup>16</sup> have exploited the atmospheric  
20 solids analysis probe technique to analyse organic compounds in secondary organic aerosol (SOA).  
21 Liquid extraction surface analysis has recently been used to analyse time-resolved aerosol samples  
22 collected onto a rotating drum impactor.<sup>17</sup> An alternative approach is to dissolve the water-soluble  
23 particle components directly using a particle-into-liquid sampler (PILS). PILS can be used to collect  
24 fractions for subsequent analysis or directly coupled with techniques such as ion chromatography<sup>18</sup> or  
25 mass spectrometry<sup>19</sup> for online analysis.

26

1 Extractive electrospray ionisation (EESI) is a new and promising technique for the online analysis of  
2 organic compounds, first introduced by Cooks et al.<sup>20</sup> In this method, a spray of charged droplets is  
3 formed by infusing a solvent mixture into a conventional ESI source. A sample flow containing  
4 analytes in the gas or particle phase is analysed by directing it into the ESI spray without prior  
5 collection on a substrate, eliminating potential offline sampling artefacts. Collision of aerosol particles  
6 with the solvent droplets extracts the soluble components from the aerosol. As solvent from the  
7 charged droplets evaporates, analyte ions are ejected into the gas phase via a Coulomb explosion  
8 mechanism<sup>21</sup> and enter the mass spectrometer for analysis.

9

10 EESI has been used to measure the composition of a diverse range of substances, including  
11 aerosolised drugs,<sup>22</sup> human breath<sup>23</sup> and olive oil.<sup>24</sup> It has also shown promise as a technique to follow  
12 the kinetics of organic chemical reactions occurring in the bulk solvent phase.<sup>25</sup> Doezema et al.<sup>26</sup>  
13 recently used EESI to detect SOA products from the ozonolysis of  $\alpha$ -pinene in both the gas and  
14 particle phase. A related technique, Ambient ESI, was recently used for molecular characterisation of  
15 gas and particle phase organic compounds and detected oligomers in SOA formed from  $\alpha$ -pinene  
16 ozonolysis.<sup>27</sup>

17

18 We report here the development of an EESI source for the real-time analysis of organic compounds in  
19 aerosol particles. The source was adapted from a commercially-available ESI source and optimised  
20 with aerosols composed of tartaric acid or oleic acid. Tartaric acid aerosol is highly functionalised and  
21 is used as a proxy for oxygenated organic compounds formed as a result of aging in the atmosphere.  
22 At low relative humidity (RH), tartaric acid could form glassy particles which are increasingly being  
23 recognised as important in the atmosphere.<sup>28</sup> Oleic acid is an unsaturated fatty acid and its reaction  
24 with ozone is well-characterised model system for organic aerosol aging.<sup>29</sup> Results from online EESI  
25 measurements of pure and oxidised particles are compared with previous offline studies.

26

## 1 **Experimental**

### 2 ***Ionisation source design and mass spectrometer description***

3 A new EESI source for online aerosol characterisation was built by adapting a commercially-available  
4 Electrospray Ionisation (ESI) source from an ion-trap mass spectrometer (Thermo Scientific Ion Max  
5 S Atmospheric Pressure Ionisation source). A custom-built aerosol injector and housing were  
6 designed for the front of the source and are illustrated in Figure 1(a).

7

8 The primary electrospray was produced by infusing solvent through a commercial electrospray probe  
9 (Thermo Scientific HESI-II). Aerosol was directed into the electrospray plume using a flexible 3 mm  
10 inner diameter PTFE tube connected to a custom aerosol nozzle (2 mm inner diameter). The housing  
11 enables the user to control the two-dimensional position and angle of the injector nozzle while the  
12 EESI source is sealed and in operation, to optimise the source for a particular application (see Figure  
13 1(a)).

14

15 The nozzle is connected via a rod to a movable plate on the outside of the housing which allows its  
16 vertical position to be set over a 20 mm range (y-displacement in Figure 1(a)). The whole plate is  
17 moved horizontally via an adjuster ring and screw thread over a 16 mm range (x-displacement in  
18 Figure 1(a)). The angle of the nozzle is controlled using a knob on the outer plate which is connected  
19 to the nozzle via a universal coupling joint and a mitre gear thread, and can be changed from 0°-90° ( $\theta$   
20 in Figure 1(a)).

21

22 Mass spectrometry measurements were made using an ion-trap mass spectrometer (Thermo Scientific  
23 LTQ Velos). The HESI-II probe was set to a spray voltage of -3.0 kV in negative ionisation mode. A  
24 water-methanol 1:1 mixture (Optima LC-MS grade solvents; Fisher Scientific) containing 0.05%

1 formic acid (90%, Breckland Scientific) was infused into the probe via syringe pump to generate the  
2 primary spray. Tandem MS experiments were performed using collision-induced dissociation (CID)  
3 by helium gas in the ion-trap using a normalised collision energy of 30%.

4

#### 5 *Aerosol production and classification*

6 Aerosol analysed by EESI was produced in the laboratory using an aerosol flow tube system which is  
7 shown in Figure 1(b).

8

9 L-Tartaric acid (99%, Aldrich) aerosol was used for the initial characterisation measurements. This  
10 was produced from solutions between 1-500 mmol/L in water (HPLC grade, Rathbones) using a  
11 custom-built nebuliser. The nebuliser was supplied with N<sub>2</sub> (oxygen-free nitrogen, BOC) at 3 bar and  
12 had an output flow rate of 1.3 L/min. The aerosol was dried using a pair of silica diffusion driers to  
13 produce an aerosol with a relative humidity (RH) below 5%.

14

15 The reaction of oleic acid (99%, Sigma) aerosol with ozone was used as a simple proof-of-principle  
16 model to study the aging of organic aerosol using EESI. This aerosol was also produced using the  
17 nebuliser from a 0.5 mmol/L solution in ethanol, with an input pressure of 2.3 bar and an output flow  
18 rate of 1 L/min. The diffusion driers and charcoal denuder were employed to remove ethanol,  
19 although small amounts were detected in the MS analysis.

20

21 Ozone was produced by flowing synthetic air (Zero Grade, BOC) through a photolysis tube  
22 containing a 185 nm UV lamp (Appleton Woods) at 0.3 L/min. The oleic acid aerosol and ozone were  
23 mixed in a 5L aerosol flow tube. The concentration of ozone after mixing was around 40ppm,

1 determined using a UV photometric ozone analyser (Thermo Scientific model 49i). A charcoal  
2 denuder was used after the flow tube to remove any remaining ozone and gas-phase organic species.

3

4 Particles from the polydisperse aerosol generated by the nebuliser were size-selected prior to EESI  
5 analysis using a differential mobility analyser (DMA) (TSI model 3081). The sheath flow rate was set  
6 to 13 L/min and the voltage was varied manually to vary the particle size transmitted. The aerosol  
7 could be humidified using a permeable Gore-Tex tube with a variable water level. 0.3 L/min of the  
8 monodisperse particle output was counted using a condensation particle counter (CPC) (TSI model  
9 3775) with the remaining 1 L/min introduced into the EESI chamber using the custom aerosol  
10 injector. Particle mass concentrations were calculated from the CPC number concentration by  
11 assuming an aerosol density from bulk literature values ( $1.8 \text{ g/cm}^3$  for tartaric acid,  $0.9 \text{ g/cm}^3$  for oleic  
12 acid) and varied between  $0.2\text{-}600 \text{ }\mu\text{g/m}^3$ .

13

14

15

16

## 1 **Results and Discussion**

### 2 ***EESI source optimisation***

3 The EESI source was built in-house and optimised to give the best combination of sensitivity and  
4 signal stability for organic aerosol measurements. The following parameters were tested: Angle and  
5 position of the aerosol nozzle ( $\theta$ , x and y, Figure 1(a)), and the sheath gas flow rate and solvent  
6 infusion flow rate of the ESI probe. The aerosol flow was held constant at 1 L/min.

7

8 It was found that maximum sensitivity was obtained when the aerosol nozzle was directed at the tip of  
9 the solvent electrospray capillary. However, this also increased the level of sample carry-over  
10 observed after the aerosol flow was switched off, probably due to particle deposition on the tip.  $\theta$  was  
11 set to  $40^\circ$  for typical operating conditions (aerosol concentration  $3\text{-}600\ \mu\text{g}/\text{m}^3$ ) so that the aerosol  
12 intersected the primary spray away from the capillary and hence sample carry-over was minimised.  
13 For the sensitive tandem MS experiments with concentrations less than  $2\ \mu\text{g}/\text{m}^3$ ,  $\theta$  was set to  $55^\circ$ .  
14 Typical values of x and y were 9 mm and 2 mm.

15

16 The sheath gas flow rate of the ESI probe was varied between 0.3-1.3 L/min by varying the supplied  
17  $\text{N}_2$  pressure. Below 0.3 L/min a stable solvent spray could not be obtained on the hour-long timescale  
18 of the EESI experiments. The most stable spray was obtained around 0.8 L/min, with higher and  
19 lower flow rates leading to more inter-scan variability and larger long-term drifts in the intensities of  
20 background signals from the solvent. Consequently, 0.8 L/min was selected for typical operating  
21 conditions (aerosol concentration  $3\text{-}600\ \mu\text{g}/\text{m}^3$ ). However, at 0.3 L/min, the EESI source was most  
22 sensitive to low concentrations of aerosol presumably because more of the incoming particles  
23 intersect the spray rather than being carried away by the sheath gas. For detecting low concentrations  
24 of aerosol, specifically the sensitive tandem MS experiments with concentrations less than  $2\ \mu\text{g}/\text{m}^3$ ,  
25 the lower sheath flow (0.3 L/min) was used.



1

2 The methanol/water/formic acid solvent mixture was infused into the HESI-II probe between 5-20  
3  $\mu\text{L}/\text{min}$  while  $\text{N}_2$  from the probe's sheath and aerosol from the injector nozzle was being delivered to  
4 the source. The spray stability was poor at 5  $\mu\text{L}/\text{min}$ , perhaps due to the additional gas flow from the  
5 injector nozzle in the source. At high flow rates of 10  $\mu\text{L}/\text{min}$  and above, a stable spray was obtained  
6 but no difference in spray stability and sensitivity could be identified in the range 10-20  $\mu\text{L}/\text{min}$ . 10  
7  $\mu\text{L}/\text{min}$  was selected to enable a longer acquisition time without refilling the syringe; coupled with a  
8 2.5 mL syringe, this enabled continuous acquisition for over 4 hours. This will be useful for future  
9 experiments using the EESI source, such as monitoring changes in the composition of aerosol from a  
10 large atmospheric simulation chamber.

11

### 12 *Characterising the optimised EESI source*

13 The optimised EESI-MS setup enabled sensitive, reproducible measurements of organic compounds  
14 in aerosol particles on long timescales. Figure 2 shows a time series where size-selected oleic acid  
15 aerosol (100 nm) was introduced into the EESI source. The MS signal corresponding to deprotonated  
16 oleic acid was closely correlated in time and intensity with the concentration of aerosol delivered to  
17 the source, as seen in Figure 2. The MS signal responded rapidly to changes in concentration,  
18 reaching a stable intensity within a matter of seconds. Increasing the aerosol concentration produced a  
19 proportional increase in the signal. Measurements of a constant aerosol source over hour-long  
20 timescales gave rise to a stable MS signal (<10% root-mean-square deviation) with negligible long-  
21 term drifts in intensity.

22

23 Sample carry-over, where a significant signal remains after the addition of new material has stopped,  
24 has been reported as a concern in other EESI experiments<sup>25</sup>. However, it is not problematic here due  
25 to the optimised operating conditions; low aerosol concentrations could be used and the nozzle

1 geometry minimised particle deposition onto the electrospray capillary and MS inlet. The signal falls  
2 back to near-baseline levels within a minute of switching aerosol for N<sub>2</sub> gas in the nozzle.

3

#### 4 ***Quantification with EESI***

5 We tested the EESI source with a range of particle concentrations and diameters to test if the  
6 extraction mechanism was dependent on particle mass, surface area or other parameters. Tartaric acid  
7 particles (<5% RH) with diameters in the range 50-250 nm were size-selected from a polydisperse  
8 aerosol distribution, using a fixed voltage on the DMA, and directed into the source. A first  
9 approximation for the total mass and surface area of the DMA's aerosol output can be made by  
10 counting the particles using a CPC and assuming a monodisperse aerosol. Tartaric acid aerosols do  
11 not effloresce and hence we assumed that they are spherical particles even at low RH. Therefore we  
12 used the aerosol's electrical mobility diameter to calculate the particle volume and then the bulk  
13 tartaric acid density to convert to a particle mass.

14

15 However assuming a monodisperse aerosol neglects the transmission of larger particles bearing  
16 multiple charges. To account for this, the full polydisperse aerosol size distribution was measured  
17 using the SMPS and so the number of particles at multiples of the selected mobility diameter could be  
18 determined. Using the equilibrium charge distributions from Wiedensohler<sup>30</sup> the fraction of doubly  
19 and triply charged particles contributing to the CPC number concentration could be estimated to give  
20 corrected mass and surface area values.

21

22 Figure 3 shows a calibration curve for tartaric acid particles with diameters between 70-200 nm after  
23 the multiple charge correction procedure. The total aerosol signal is dependent only on the mass of  
24 aerosol and is independent of particle size. This again points to a mechanism where particles are fully  
25 dissolved in the spray regardless of size. Large particles leave no undissolved "core". Presumably

1 above a certain particle diameter such a phenomenon will occur, but it appears that this is unlikely to  
2 be problematic for sub-micrometer aerosols.

3

4 Measurements mostly focused on lower aerosol concentrations below  $100 \mu\text{g}/\text{m}^3$ . This range is typical  
5 for laboratory atmospheric chamber studies (although such particles will contain many compounds  
6 and hence the concentrations of individual species will be lower). The few higher concentrations  
7 demonstrate that the technique has a linear dynamic range over the entire concentration range tested  
8 ( $3\text{-}600 \mu\text{g}/\text{m}^3$ ). This represents the first quantification of an aerosol component using an online ESI  
9 technique; the data suggest that EESI-MS could be used in a semi-quantitative fashion for known  
10 analytes down to a concentration of a few  $\mu\text{g}/\text{m}^3$ . Authors describing the related AESI technique were  
11 unable to quantify particle components in its current configuration owing to instabilities in the mass  
12 analyser used.<sup>27</sup>

13

14 The charge correction procedure described above was applied to all of the data points in the 70, 100  
15 and 200 nm series in Figure 4. Explicit charge correction was not performed as described above for all  
16 of the data points in the 150nm series due to the time consuming requirement of measuring full  
17 aerosol size distributions for each nebuliser solution concentration (i.e. each data point). Instead, size  
18 distributions for most concentrations were interpolated from four solution concentrations which were  
19 explicitly corrected. The interpolation procedure appears to have been successful and the 150nm data  
20 show good agreement with the other diameters. The fractions of multiply charged particles  
21 contributing to the CPC number count in figure 6 was also estimated using this interpolation method.

22

23 Previous studies have indicated that EESI is capable of analysing samples with complex matrices  
24 which suffer large ion suppression and loss of detector sensitivity using direct infusion ESI  
25 techniques.<sup>20,31</sup> Here, we further minimise possible ion-suppression phenomena by employing

1 relatively low analyte concentrations; this means that the availability of primary spray droplets to  
2 dissolve and ionise the aerosol particles should not be a limiting factor in analyte ion formation. As a  
3 result, changes in the intensity of ions over time are likely to correlate with concentration changes of  
4 analytes in particles, as seen for a simple case in Figure 2. It should be noted, however, that our  
5 testing has been limited to particles composed of organic compounds and so the influence of a  
6 complex particle matrix (particularly the presence of inorganic salts) has not been assessed.

7

### 8 ***Tandem MS measurements***

9 The data in Figure 3 have a constant background signal of  $1.2 \times 10^4$  counts at  $m/z$  149 which has been  
10 subtracted. This signal appears to originate from the “pure” solvent used for the primary ESI spray  
11 and is observed even when no aerosol is added to the source. It presents a problem when analysing  
12 low aerosol concentrations because the signal from the aerosol analyte is comparable to the  
13 background; this ultimately determines the technique’s limit of detection. The resolution and mass  
14 accuracy of the LTQ Velos mass spectrometer are not sufficient to assign the background peak to a  
15 particular compound, and indeed it seems likely that the signal may originate from a mixture of  
16 unresolved compounds in the solvent. Extensive cleaning of the HESI-II probe does not reduce this  
17 signal, suggesting it is not from tartaric acid particles deposited on the probe in previous experiments.

18

19 The way we overcome this issue, and hence reduce the limit of detection, is to perform tandem MS  
20 measurements on the combined aerosol and background ions which make up the observed  $m/z$  149  
21 signal. Briefly, tandem MS involves isolating ions in a small mass window (typically 1  $m/z$ ) from the  
22 full spectrum and discarding all ions which fall outside of this window. The remaining isolated ions  
23 are fragmented using a collision gas; different ions will have different characteristic fragmentation  
24 patterns depending on their molecular structure. By monitoring fragments unique to the analyte of  
25 interest it is possible to resolve them from background impurities which have the same parent ion  $m/z$ ,  
26 but form different  $m/z$  fragments.

1

2 This principle is applied to tartaric acid aerosol in figure 5. Spectrum (a) shows the fragments formed  
3 from the tandem MS of the solvent background in the range  $m/z$  148.5-149.5. Major fragments are  
4 observed at  $m/z$  77, 105 and 121. When tartaric acid aerosol was added at a concentration of  $1\mu\text{g}/\text{m}^3$   
5 (spectrum (b)), new peaks appear in the tandem MS spectrum at  $m/z$  59, 87, 103 and 131. The  
6 molecular formulae of these peaks are assigned in (c) at a higher aerosol concentration ( $20\mu\text{g}/\text{m}^3$ )  
7 where they become the dominant peaks. They were confirmed as tartaric acid fragments by direct  
8 infusion of a tartaric acid standard solution into an ultrahigh resolution LTQ Orbitrap Velos mass  
9 spectrometer, where unambiguous molecular compositions could be assigned.

10

11 The signal from the most intense fragment peak from tartaric acid,  $m/z$  103, is plotted as a function of  
12 tartaric acid aerosol mass concentration in figure 6. It varies linearly with concentration and extends  
13 the dynamic range of the EESI technique below  $1\mu\text{g}/\text{m}^3$  for known analytes. The other assigned  
14 fragments also vary linearly with mass concentration. The error bars on the data correspond to the  
15 standard deviation of the scan-to-scan variability (which we believe arises primarily from variations in  
16 the primary ESI spray). For the lowest aerosol concentration tested,  $0.22\mu\text{g}/\text{m}^3$ , the signal is 2.5 times  
17 the background signal from the solvent and is easily distinguished from the inter-scan variability. This  
18 probably represents an upper bound on the limit of detection for tartaric acid.

19

20 The limit of detection using this method will depend on the particular analyte under consideration due  
21 to differences in its ionisation probability and fragmentation pattern. However, it demonstrates that in  
22 general EESI-MS/MS will be highly sensitive to small changes in the concentration of analytes in  
23 particles and that detection limits in the sub- $\mu\text{g}/\text{m}^3$  range can be achieved.

24

25 *Effect of aerosol phase and water content*

1 To examine the extraction mechanism, we tested the impact of aerosol water content on the extraction  
2 efficiency of the EESI process. This was achieved by humidifying the dried aerosol after it was size-  
3 selected in the DMA, to ensure that the mass of analyte in the particles remained constant. Tartaric  
4 acid and maleic acid aerosols were tested, both of which are hygroscopic and in principle fully soluble  
5 in the primary spray. The two compounds exhibit different phase behaviour; maleic acid effloresces to  
6 form a crystalline solid during the drying process and deliquesces around 87% RH<sup>32</sup> – we use it to test  
7 extraction of solid soluble particles. Tartaric acid does not effloresce and a small amount of water,  
8 10% by mass,<sup>33</sup> remains associated with the particle at low RH.

9  
10 Figure xx\*\*\* shows the relative extraction efficiencies of maleic and tartaric acid aerosols (dry  
11 diameter 150 nm) as a function of relative humidity. The extraction efficiencies were calculated by  
12 scaling the observed MS signal to the mass of aerosol estimated from the number of particles detected  
13 by the CPC. This mass estimate is somewhat uncertain due to the presence of multiply charged  
14 particles. We found the loss of (positively charged) size-selected particles through the humidification  
15 setup to be large and strongly RH-dependent. It has been shown that particle losses are also size and  
16 charge dependent<sup>34</sup> so the contribution of large multiply-charged particles to the MS signal could not  
17 be accounted for.

18  
19 Despite this uncertainty, the EESI mechanism is able to detect both solid and aqueous organic  
20 particles and there does not appear to be a systematic trend in the extraction efficiency as a function of  
21 liquid water content. We infer a mechanism where soluble solid particles are fully dissolved and  
22 extracted into the solvent spray. This finding will be important when analysing aerosols from  
23 chambers; evidence suggests that these may form amorphous solid phases as a result of aging  
24 processes<sup>35</sup>.

25

1 It should be emphasized that the particles must be in principle soluble in the electrospray solvent to be  
2 detected using EESI. We do not expect to detect insoluble particles such as elemental carbon and  
3 mineral dust. However, we are unsure how mixed particles containing both soluble and insoluble  
4 fractions affect the EESI ionisation mechanism.

5

### 6 *Chemistry of a model system – oleic acid oxidation*

7 To test the applicability of EESI-MS to laboratory studies of aerosol aging, a proof-of-principle  
8 experiment involving the ozonolysis of oleic acid particles was conducted. Oleic acid aerosol is a  
9 well-characterised model system for organic aerosol in the atmosphere and its reaction products have  
10 been extensively studied in this group as well as others.<sup>36–38</sup>

11

12 Figure 7 shows mass spectra acquired using EESI of oleic acid aerosol at a concentration of 20  $\mu\text{g}/\text{m}^3$ ,  
13 before and after ozonolysis. The spectra shown are background subtracted; a “solvent background”  
14 spectrum was acquired by flowing pure  $\text{N}_2$  through the aerosol nozzle, and this was subtracted from  
15 the raw aerosol spectra. The unoxidised oleic acid particles show only one major peak in the negative  
16 mode, at  $m/z$  281, which is deprotonated oleic acid (OA). The peak at  $m/z$  327 corresponds to a non-  
17 covalent adduct between oleic acid and ethanol, suggesting that there is a small amount of ethanol  
18 remaining in the particles originating from the particle generation process.

19

20 By contrast, a variety of oxidation products can be observed in the oleic acid particles processed by  
21 ozone (40 ppm, 3 minute reaction time) and the major peaks can be assigned to known reaction  
22 products. Oleic acid is an 18-carbon fatty acid containing a single double bond and so ozonolysis via a  
23 Criegee intermediate mechanism leads to the formation of four 9-carbon primary reaction products.  
24 This chemistry has been characterised in detail elsewhere.<sup>36–38</sup> The peaks at  $m/z$  157, 171 and 187  
25 correspond to three of the primary oxidation products; nonanoic acid (NA), 9-oxonanoic acid (ON)

1 and azaleic acid (AA) respectively. The fourth product, nonanal, has a high vapour pressure and so  
2 partitions out of the particle and into the gas phase. Since a charcoal denuder was used in this  
3 experiment to remove unreacted ozone and volatile organic compounds, nonanal was not observed  
4 here. Unreacted OA can be seen as a consequence of the short residence time of the aerosol in the  
5 flow tube reactor. Adducts of OA and the major products with ethanol can again be seen.

6

7 A number of the smaller peaks can also be assigned. The ozonolysis mechanism discussed above  
8 involves the formation of a Criegee intermediate (CI), a highly reactive biradical species. A possible  
9 fate of the CI is to react with the primary reaction products or unreacted oleic acid to form high  
10 molecular weight oligomer chains. The peak at  $m/z$  375 is consistent with a CI adding to AA to form  
11 a covalently-bonded dimer. Measurements at higher aerosol concentrations ( $100 \mu\text{g}/\text{m}^3$ ) reveal a  
12 variety of dimers, trimers and higher oligomers which were reported and characterised in detail using  
13 offline analysis methods.<sup>36,37,39</sup>

14

### 15 *Implications*

16 The new extractive electrospray ionisation (EESI-MS) source developed and thoroughly characterised  
17 here offers a number of advantages for the online characterisation of organic aerosol composition.  
18 EESI produces intact molecular ions with little fragmentation because of the “soft” extraction and  
19 ionisation process. Hence, characterisation of the molecular composition of highly complex mixtures  
20 such as aerosols is simpler than for other online techniques. This will enable the elucidation of aerosol  
21 reaction mechanisms in unprecedented detail with high time resolution.

22

23 New insight into the EESI extraction mechanism will help to better quantify processes occurring in  
24 aerosols. We demonstrated that the dynamic range for quantification of the method covers more than  
25 three orders of magnitude ( $0.2\text{-}600 \mu\text{g}/\text{m}^3$ ) which will enable the analysis of particle composition



1 under ambient conditions. Particle concentration changes were detected on the timescale of seconds  
2 and the technique shows promise for characterising the time evolution of aerosol composition in real  
3 time. Future work will attempt to understand the mechanisms and reaction kinetics occurring in  
4 particles by monitoring changes in the composition of aerosols in laboratory flow tube and chamber  
5 studies.

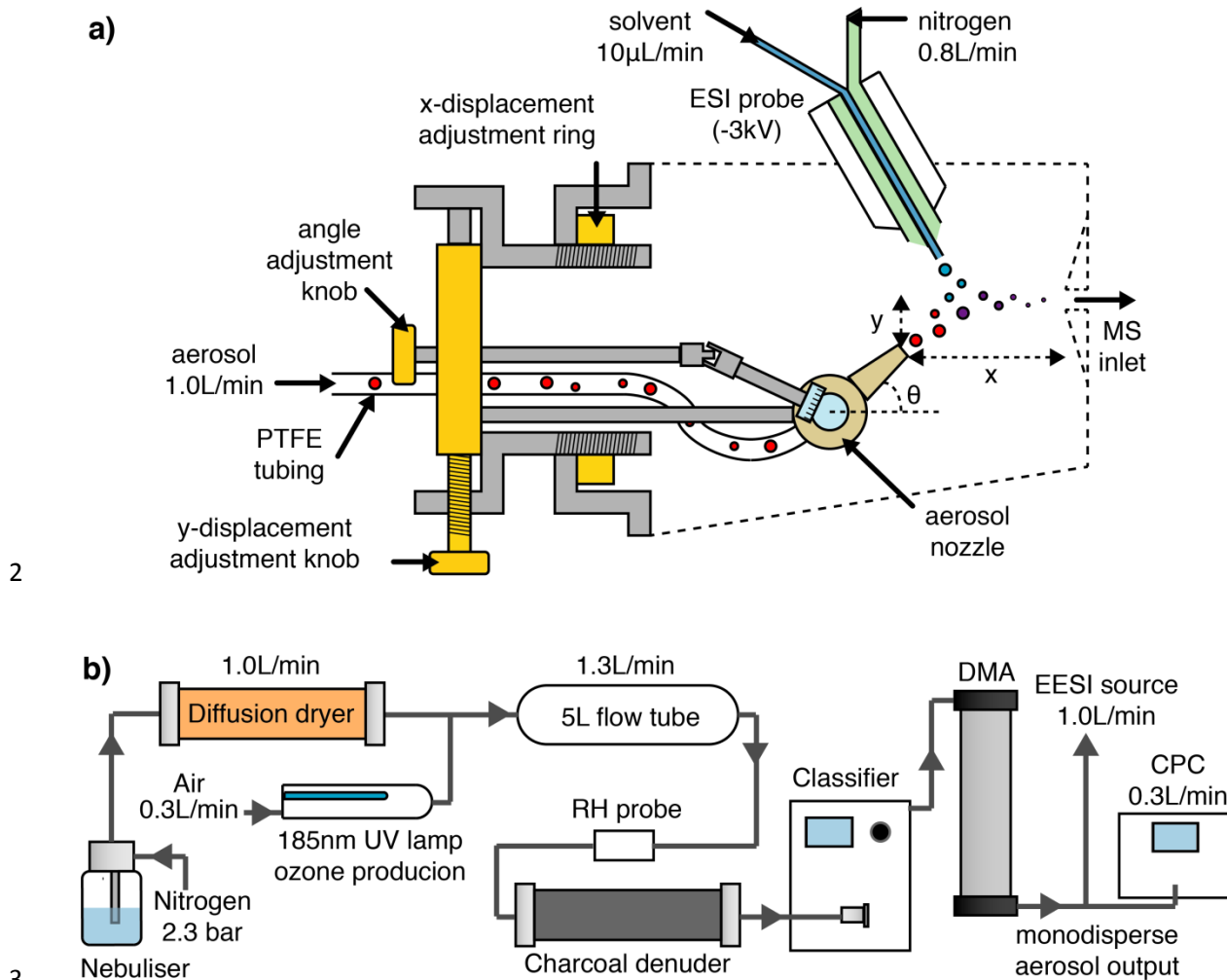
6

## 7 **Acknowledgements**

8 Financial support by the UK Natural Environment Research Council (NERC) is greatly  
9 acknowledged.

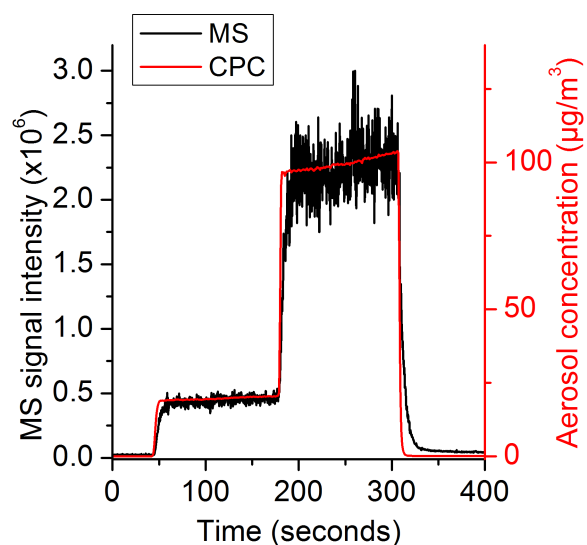
10

1 **Figures**



4 Figure 1: (a) Design for the custom-built Extractive Electrospray Ionisation source. The housing was  
 5 adapted from a Thermo Ion Max API source (dotted line) fitted with an electrospray probe (HESI-II).  
 6 The aerosol particles (red) are directed into a spray of charged solvent droplets (blue) where  
 7 extraction and ionisation of the aerosol analytes occurs (purple) and the solvent evaporates to eject  
 8 analyte ions into the gas phase. The geometric parameters x, y and  $\theta$  can be optimised during source  
 9 operation. (b) Schematic diagram of the aerosol flow tube and size-selection apparatus for the  
 10 oxidation of oleic acid aerosol. For tartaric acid, the ozone lamp was not used and the nitrogen  
 11 pressure for the nebuliser was increased to 3 bar to maintain a total flow rate of 1.3 L/min. DMA –  
 12 differential mobility analyser, CPC – condensation particle counter.

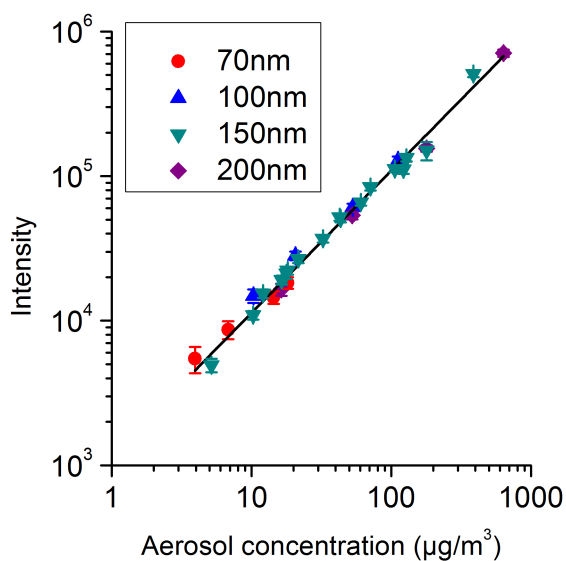
13



1

2 Figure 2: Red line: Time series of the mass concentration of oleic acid aerosol delivered to the EESI  
 3 source, measured using a condensation particle counter (CPC). Black line: Time series of the MS  
 4 signal at  $m/z$  281 corresponding to deprotonated oleic acid in negative ionisation mode. All ion source  
 5 parameters were held constant. The inter-scan noise scales approximately with the signal intensity.  
 6 The signal/noise ratio (i.e. average/standard deviation) of the MS signal was 10.3 between 0-40  
 7 seconds, 14.3 between 80-160 seconds and 11.6 between 200-280 seconds.

8

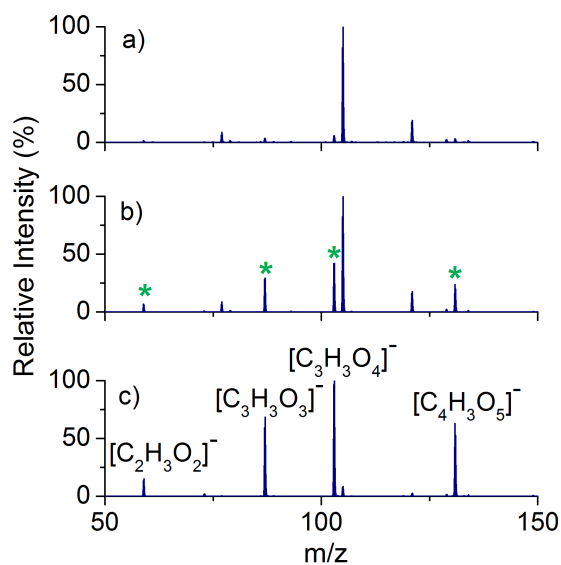


1

2 Figure 3: The signal intensity of tartaric acid ( $m/z$  149), linearly correlated with the total particle mass  
 3 concentration between  $3\text{-}600\mu\text{g}/\text{m}^3$ . For each diameter, the particle concentration was varied by using  
 4 different concentrations of tartaric acid solution in the nebuliser. Over the range of diameters between  
 5 70-200 nm the extraction efficiency is independent of particle size. The data were corrected to  
 6 account for the transmission of multiply charged particles through the DMA and a background solvent  
 7 signal of  $1.2 \times 10^4$  counts was subtracted from all data points.

8

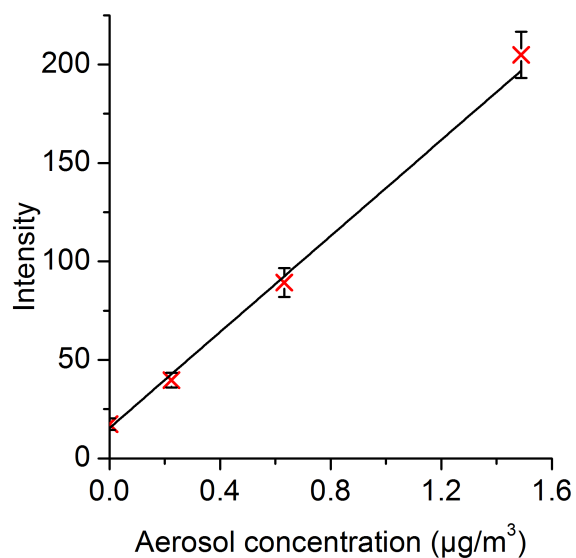
9



1

2 Figure 5: Mass spectra showing tandem MS fragmentation measurements on the m/z 149 peak. (a)  
 3 solvent background without aerosol; (b) 1  $\mu\text{g}/\text{m}^3$  tartaric acid aerosol, where new fragments (\*) appear  
 4 at m/z 59, 87, 103 and 131 (c) 20  $\mu\text{g}/\text{m}^3$  aerosol, showing the fragments at correspondingly higher  
 5 intensities relative to the background. Peak assignments in (c) were confirmed by direct infusion of a  
 6 tartaric acid standard solution into an ultrahigh-resolution LTQ Orbitrap Velos mass spectrometer  
 7 with sufficient mass accuracy and resolving power to unambiguously assign the molecular formulae  
 8 of the ions.

9



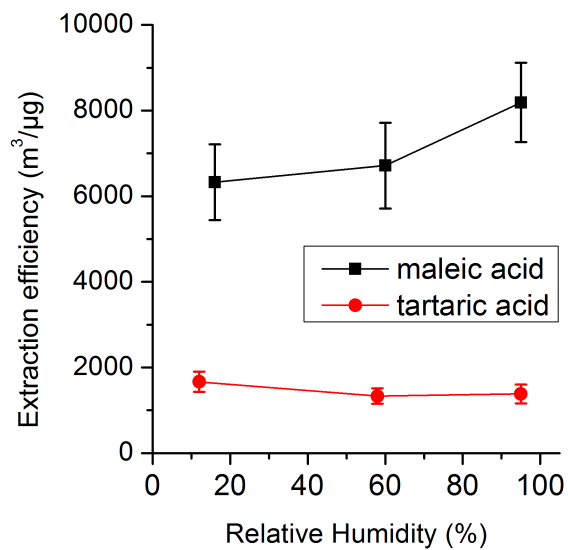
1

2 Figure 6: MS signal at  $m/z$  103 for tandem MS fragmentation of the  $m/z$  149 peak, as a function of  
3 tartaric acid aerosol concentration.  $m/z$  103 was identified as the most intense fragment of the tartaric  
4 acid parent ion in figure 5. The  $m/z$  149 ions were fragmented using collision induced dissociation  
5 (CID) in the ion trap of the mass spectrometer. The error bars represent the standard deviation of the  
6 average intensity of 100 scans.

7

8

9



1

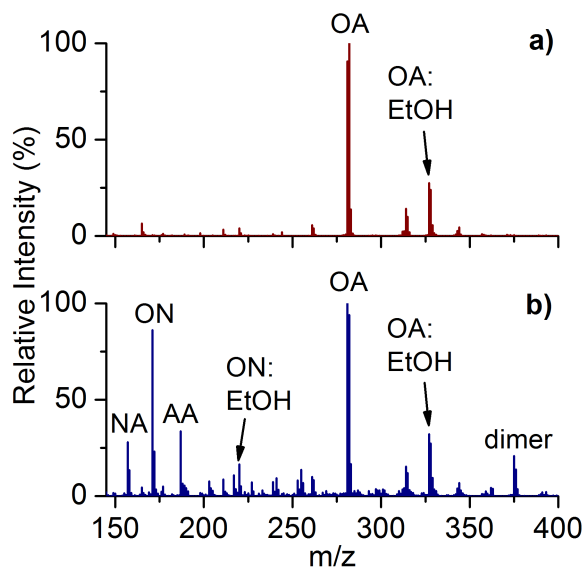
2 Figure 7\*\*\*: Extraction of organic aerosol particles by EESI as a function of relative humidity.

3 Extraction efficiency was calculated by dividing the MS intensity by the aerosol mass concentration

4 estimated from the CPC. Within experimental uncertainty, there was no significant trend in the

5 extraction efficiency as a function of relative humidity for either compound. Lines joining the data

6 points are as a guide to the eye.



1

2 Figure 8\*\*\*: Mass spectra between m/z 150-450 showing: (a) 20  $\mu\text{g}/\text{m}^3$  oleic acid aerosol nebulised  
 3 from a 0.5 mM solution in ethanol. (b) 20  $\mu\text{g}/\text{m}^3$  aerosol oxidised by 40 ppm ozone for 3 minutes,  
 4 showing the major reaction products and some unreacted oleic acid.

5

6

7



## 1 References

- 2 (1) Solomon, S.; Qin, D.; Manning, M.; Chen, Z.; Averyt, K.; Tignor, M.; Miller, H. IPCC  
3 2007: Summary for Policymakers. In *Climate Change 2007: The Physical Science*  
4 *Basis*; 2007.
- 5 (2) Dominici, F.; Peng, R. D.; Bell, M. L.; Pham, L.; McDermott, A.; Zeger, S. L.; Samet,  
6 J. M. Fine particulate air pollution and hospital admission for cardiovascular and  
7 respiratory diseases. *The Journal of the American Medical Association* **2006**, *295*,  
8 1127–34.
- 9 (3) Pope, C. A.; Ezzati, M.; Dockery, D. W. Fine-particulate air pollution and life  
10 expectancy in the United States. *The New England Journal of Medicine* **2009**, *360*,  
11 376–86.
- 12 (4) Jimenez, J. L.; Canagaratna, M. R.; Donahue, N. M.; Prevot, A. S. H.; Zhang, Q.;  
13 Kroll, J. H.; DeCarlo, P. F.; Allan, J. D.; Coe, H.; Ng, N. L.; Aiken, A. C.; Docherty,  
14 K. S.; Ulbrich, I. M.; Grieshop, A. P.; Robinson, A. L.; Duplissy, J.; Smith, J. D.;  
15 Wilson, K. R.; Lanz, V. A.; Hueglin, C.; Sun, Y. L.; Tian, J.; Laaksonen, A.;  
16 Raatikainen, T.; Rautiainen, J.; Vaattovaara, P.; Ehn, M.; Kulmala, M.; Tomlinson, J.  
17 M.; Collins, D. R.; Cubison, M. J.; Dunlea, E. J.; Huffman, J. A.; Onasch, T. B.;  
18 Alfarra, M. R.; Williams, P. I.; Bower, K.; Kondo, Y.; Schneider, J.; Drewnick, F.;  
19 Borrmann, S.; Weimer, S.; Demerjian, K.; Salcedo, D.; Cottrell, L.; Griffin, R.;  
20 Takami, A.; Miyoshi, T.; Hatakeyama, S.; Shimono, A.; Sun, J. Y.; Zhang, Y. M.;  
21 Dzepina, K.; Kimmel, J. R.; Sueper, D.; Jayne, J. T.; Herndon, S. C.; Trimborn, A. M.;  
22 Williams, L. R.; Wood, E. C.; Middlebrook, A. M.; Kolb, C. E.; Baltensperger, U.;  
23 Worsnop, D. R. Evolution of organic aerosols in the atmosphere. *Science* **2009**, *326*,  
24 1525–9.
- 25 (5) Kanakidou, M.; Seinfeld, J. H.; Pandis, S. N.; Barnes, I.; Dentener, F. J.; Facchini, M.  
26 C.; Van Dingenen, R.; Ervens, B.; Nenes, a.; Nielsen, C. J.; Swietlicki, E.; Putaud, J.  
27 P.; Balkanski, Y.; Fuzzi, S.; Horth, J.; Moortgat, G. K.; Winterhalter, R.; Myhre, C. E.  
28 L.; Tsigaridis, K.; Vignati, E.; Stephanou, E. G.; Wilson, J. Organic aerosol and global  
29 climate modelling: a review. *Atmospheric Chemistry and Physics* **2005**, *5*, 1053–1123.
- 30 (6) Chen, Q.; Liu, Y.; Donahue, N. M.; Shilling, J. E.; Martin, S. T. Particle-Phase  
31 Chemistry of Secondary Organic Material: Modeled Compared to Measured O:C and  
32 H:C Elemental Ratios Provide Constraints. *Environmental Science & Technology*  
33 **2011**.
- 34 (7) Hamilton, J. F.; Webb, P. J.; Lewis, A. C.; Hopkins, J. R.; Smith, S.; Davy, P. Partially  
35 oxidised organic components in urban aerosol using GCXGC-TOF/MS. *Atmospheric*  
36 *Chemistry and Physics* **2004**, *4*, 1279–1290.
- 37 (8) Jayne, J. T.; Leard, D. C.; Zhang, X.; Davidovits, P.; Smith, K. A.; Kolb, C. E.;  
38 Worsnop, D. R. Development of an Aerosol Mass Spectrometer for Size and  
39 Composition Analysis of Submicron Particles. *Aerosol Science & Technology* **2000**,  
40 *33*, 49–70.

- 1 (9) Silva, P. J.; Prather, K. A. Interpretation of Mass Spectra from Organic Compounds in  
2 Aerosol Time-of-Flight Mass Spectrometry. *Analytical Chemistry* **2000**, *72*, 3553–  
3 3562.
- 4 (10) Geddes, S.; Nichols, B.; Todd, K.; Zahardis, J.; Petrucci, G. A. Near-infrared laser  
5 desorption/ionization aerosol mass spectrometry for measuring organic aerosol at  
6 atmospherically relevant aerosol mass loadings. *Atmospheric Measurement Techniques*  
7 **2010**, *3*, 1175–1183.
- 8 (11) Öktem, B.; Tolocka, M. P.; Johnston, M. V. On-Line Analysis of Organic Components  
9 in Fine and Ultrafine Particles by Photoionization Aerosol Mass Spectrometry. **2004**,  
10 *76*, 253–261.
- 11 (12) Vogel, A. L.; Äijälä, M.; Brüggemann, M.; Ehn, M.; Junninen, H.; Petäjä, T.;  
12 Worsnop, D. R.; Kulmala, M.; Williams, J.; Hoffmann, T. Online atmospheric pressure  
13 chemical ionization ion trap mass spectrometry (APCI-IT-MSn) for measuring organic  
14 acids in concentrated bulk aerosol – a laboratory and field study. *Atmospheric*  
15 *Measurement Techniques Discussions* **2012**, *5*, 6147–6182.
- 16 (13) Hoffmann, T.; Huang, R.-J.; Kalberer, M. Atmospheric Analytical Chemistry.  
17 *Analytical Chemistry* **2011**.
- 18 (14) Bateman, A. P.; Walser, M. L.; Desyaterik, Y.; Laskin, J.; Laskin, A.; Nizkorodov, S. a  
19 The effect of solvent on the analysis of secondary organic aerosol using electrospray  
20 ionization mass spectrometry. *Environmental Science & Technology* **2008**, *42*, 7341–6.
- 21 (15) Laskin, J.; Laskin, A.; Roach, P. J.; Slysz, G. W.; Anderson, G. A.; Nizkorodov, S. A.;  
22 Bones, D. L.; Nyugen, L. Q. High-Resolution Desorption Electrospray Ionization Mass  
23 Spectrometry for Chemical Characterization of Organic Aerosols. *Analytical*  
24 *Chemistry* **2010**, *82*, 2048–2058.
- 25 (16) Bruns, E. A.; Greaves, J.; Finlayson-Pitts, B. J. Atmospheric Solids Analysis Probe  
26 Mass Spectrometry : A New Approach for Airborne Particle Analysis. *Analytical*  
27 *Chemistry* **2010**, *82*, 5922–5927.
- 28 (17) Fuller, S. J.; Zhao, Y.; Cliff, S. S.; Wexler, A. S.; Kalberer, M. Direct Surface Analysis  
29 of Time-Resolved Aerosol Impactor Samples with Ultrahigh-Resolution Mass  
30 Spectrometry. **2012**.
- 31 (18) Orsini, D. a.; Ma, Y.; Sullivan, A.; Sierau, B.; Baumann, K.; Weber, R. J. Refinements  
32 to the particle-into-liquid sampler (PILS) for ground and airborne measurements of  
33 water soluble aerosol composition. *Atmospheric Environment* **2003**, *37*, 1243–1259.
- 34 (19) Bateman, A. P.; Nizkorodov, S. A.; Laskin, J.; Laskin, A. High-Resolution  
35 Electrospray Ionization Mass Spectrometry Analysis of Water-Soluble Organic  
36 Sampler †. *Analytical Chemistry* **2010**, *82*, 8010–8016.
- 37 (20) Chen, H.; Venter, A.; Cooks, R. G. Extractive electrospray ionization for direct  
38 analysis of undiluted urine, milk and other complex mixtures without sample  
39 preparation. *Chemical Communications* **2006**, 2042–4.

- 1 (21) Kebarle, P.; Peschke, M. On the mechanisms by which the charged droplets produced  
2 by electrospray lead to gas phase ions. *Analytica Chimica Acta* **2000**, *406*, 11–35.
- 3 (22) Gu, H.; Hu, B.; Li, J.; Yang, S.; Han, J.; Chen, H. Rapid analysis of aerosol drugs  
4 using nano extractive electrospray ionization tandem mass spectrometry. *Analyst* **2010**,  
5 *135*, 1259–67.
- 6 (23) Chen, H.; Wortmann, A.; Zhang, W.; Zenobi, R. Rapid in vivo fingerprinting of  
7 nonvolatile compounds in breath by extractive electrospray ionization quadrupole  
8 time-of-flight mass spectrometry. *Angewandte Chemie (International ed. in English)*  
9 **2007**, *46*, 580–3.
- 10 (24) Law, W. S.; Chen, H. W.; Balabin, R.; Berchtold, C.; Meier, L.; Zenobi, R. Rapid  
11 fingerprinting and classification of extra virgin olive oil by microjet sampling and  
12 extractive electrospray ionization mass spectrometry. *Analyst* **2010**, *135*, 773–8.
- 13 (25) McCullough, B. J.; Bristow, T.; O'Connor, G.; Hopley, C. On-line reaction monitoring  
14 by extractive electrospray ionisation. *Rapid Communications in Mass Spectrometry*  
15 **2011**, *25*, 1445–51.
- 16 (26) Doezema, L. A.; Longin, T.; Cody, W.; Perraud, V.; Dawson, M. L.; Ezell, M. J.;  
17 Greaves, J.; Johnson, K. R.; Finlayson-Pitts, B. J. Analysis of secondary organic  
18 aerosols in air using extractive electrospray ionization mass spectrometry (EESI-MS).  
19 *RSC Advances* **2012**, *2*, 2930.
- 20 (27) Horan, A. J.; Gao, Y.; Iv, W. A. H.; Johnston, M. V Online Characterization of  
21 Particles and Gases with an Ambient Electrospray Ionization Source. *Analytical*  
22 *Chemistry* **2012**, *84*, 9253–9258.
- 23 (28) Zobrist, B.; Marcolli, C.; Pedernara, D. A.; Koop, T. Do atmospheric aerosols form  
24 glasses? *Atmospheric Chemistry and Physics* **2008**, *8*, 5221–5244.
- 25 (29) Zahardis, J.; Petrucci, G. A. The oleic acid-ozone heterogeneous reaction system:  
26 products, kinetics, secondary chemistry, and atmospheric implications of a model  
27 system – a review. *Atmospheric Chemistry and Physics* **2007**, *7*, 1237–1274.
- 28 (30) Wiedensohler, A. An approximation of the bipolar charge distribution for particles in  
29 the submicron size range. *Journal of Aerosol Science* **1988**, *19*, 387–389.
- 30 (31) Law, W. S.; Wang, R.; Hu, B.; Berchtold, C.; Meier, L.; Chen, H.; Zenobi, R. On the  
31 mechanism of extractive electrospray ionization. *Analytical Chemistry* **2010**, *82*, 4494–  
32 500.
- 33 (32) Pope, F. D.; Gallimore, P. J.; Fuller, S. J.; Cox, R. A.; Kalberer, M. Ozonolysis of  
34 maleic acid aerosols: effect upon aerosol hygroscopicity, phase and mass.  
35 *Environmental Science & Technology* **2010**, *44*, 6656–60.
- 36 (33) Peng, C.; Chan, M. N.; Chan, C. K. The hygroscopic properties of dicarboxylic and  
37 multifunctional acids: measurements and UNIFAC predictions. *Environmental Science*  
38 *& Technology* **2001**, *35*, 4495–4501.

- 1 (34) Barat, R. B.; Callahan, V. L.; Cedio-Fengya, D. J.; Stevens, J. G. The effect of particle  
2 size distribution on the deposition of charged particles in tubes. *Advances in*  
3 *Environmental Research* **2002**, *7*, 105–115.
- 4 (35) Virtanen, A.; Joutsensaari, J.; Koop, T.; Kannosto, J.; Yli-Pirilä, P.; Leskinen, J.;  
5 Mäkelä, J. M.; Holopainen, J. K.; Pöschl, U.; Kulmala, M.; Worsnop, D. R.;  
6 Laaksonen, A. An amorphous solid state of biogenic secondary organic aerosol  
7 particles. *Nature* **2010**, *467*, 824–7.
- 8 (36) Lee, J. W. L.; Carrascón, V.; Gallimore, P. J.; Fuller, S. J.; Björkegren, A.; Spring, D.  
9 R.; Pope, F. D.; Kalberer, M. The effect of humidity on the ozonolysis of unsaturated  
10 compounds in aerosol particles. *Physical chemistry chemical physics : PCCP* **2012**, *14*,  
11 8023–31.
- 12 (37) Ziemann, P. J. Aerosol products, mechanisms, and kinetics of heterogeneous reactions  
13 of ozone with oleic acid in pure and mixed particles. *Faraday Discussions* **2005**, *130*,  
14 469–490.
- 15 (38) Vesna, O.; Sax, M.; Kalberer, M.; Gaschen, A.; Ammann, M. Product study of oleic  
16 acid ozonolysis as function of humidity. *Atmospheric Environment* **2009**, *43*, 3662–  
17 3669.
- 18 (39) Reynolds, J. C.; Last, D. J.; McGillen, M.; Nijs, A.; Horn, A. B.; Percival, C.;  
19 Carpenter, L. J.; Lewis, A. C. Structural analysis of oligomeric molecules formed from  
20 the reaction products of oleic acid ozonolysis. *Environmental Science & Technology*  
21 **2006**, *40*, 6674–81.

22